Available online at www.sciencedirect.com
ScienceDirect
Applied Catalysis B: Environmental 79 (2008) 341–346
APPLIED CATALYSIS B: ENVIRONMENTAL
www.elsevier.com/locate/apcatb

Electrocatalysis of ethanol oxidation on Pt monolayers deposited on carbon-supported Ru and Rh nanoparticles

F.H.B. Lima *, E.R. Gonzalez

Instituto de Química de São Carlos, Universidade de São Paulo, CEP 13560-970, CP 780 São Carlos, SP, Brazil

Received 25 July 2007; received in revised form 23 October 2007; accepted 26 October 2007
Available online 4 November 2007

Abstract

Pt monolayers deposited on carbon-supported Ru and Rh nanoparticles were investigated as electrocatalysts for ethanol oxidation. Electronic features of the Pt monolayers were studied by *in situ* XANES (X-ray absorption near-edge structure). The electrochemical activity was investigated by cyclic voltammetry and cronoamperometric experiments. Spectroscopic and electrochemical results were compared to those obtained on carbon-supported Pt–Ru and Pt–Rh alloys, and Pt E-TEK. XAS results indicate a modification of the Pt 5d band due to geometric and electronic interactions with the Ru ant Rh substrates, but the effect of withdrawing electrons from Pt is less pronounced in relation to that for the corresponding alloys. Electrochemical stripping of adsorbed CO, which is one of the intermediates, and the currents for the oxidation of ethanol show faster kinetics on the Pt monolayer deposited on Ru nanoparticles, and an activity that exceeds that of conventional catalysts with much larger amounts of platinum.

Keywords: Ethanol electro-oxidation; Platinum–ruthenium alloy; Platinum–rhodium alloy; Pt monolayer

1. Introduction

Many works have been carried out in recent years aiming at increasing the electrocatalytic activity of platinum for the electro-oxidation of ethanol, and also of CO, which is one of the adsorbed intermediates, for fuel cell applications [1–7]. Pt–Ru alloy catalysts showed an enhanced CO electro-oxidation kinetics compared to pure Pt, and this fact has been attributed to: (1) the bi-functional mechanism [8], and (2) the electronic effect [9] induced by the electronic interaction between Pt and Ru, enhancing the oxidation of the adsorbed CO intermediate at the metal surface. The electro-oxidation of ethanol undergoes parallel reactions, producing acetaldehyde, acetic acid and CO_2. The pathways seem to be also sensitive to the alloying non-noble metal, which influences the bi-functional mechanism and the electronic effect (ligand effect).

A shift of the d-band center has been calculated for alloys with two or more metals, or for surface segregated phases of a given metal on a metal nanoparticle [10–13]. In the case of alloying Pt with Ru and/or Rh, or in surface segregated Pt on these substrates, there is a down-shift of the Pt 5 d-band center. This is mainly caused by the lattice mismatch and the strong electronic interaction between Pt and Ru and/or Rh atoms [11], leading to a reduced adsorption strength of absorbates on the Pt surface.

Thus, for ethanol electro-oxidation, and in addition to the bi-functional mechanism, different activities of the Pt alloys compared to pure Pt are expected when the Pt 5d band center shifts. This may cause a variation of the adsorption strength of the reaction intermediates, leading, eventually, to different reaction products. The present work evaluates the electrocatalytic activity for ethanol electro-oxidation on a Pt monolayer deposited on carbon-supported Ru and Rh nanoparticles. The electrochemical activity of these catalysts, which contain much less platinum than the conventional catalysts, is correlated with their electronic properties, and compared to the results obtained on carbon-supported Pt–Ru and Pt–Rh alloys and on Pt E-TEK.

2. Experimental

Carbon-supported Ru and Rh nanoparticles, represented as Ru/C and Rh/C, used as substrate for the Pt monolayer, were prepared by impregnating a high surface area carbon (Vulcan

* Corresponding author. Tel.: +55 16 3373 9934; fax: +55 16 3373 9952.
E-mail address: fabiohbl@gmail.com (F.H.B. Lima).

0926-3373/$ – see front matter © 2007 Elsevier B.V. All rights reserved.
doi:10.1016/j.apcatb.2007.10.028

XC-72R), with a solution of $RuCl_3$ or $RhCl_3$ under sonication for 10 min, and dried by evaporation of the water in a petri plate at 80 °C. The resulting powders were 20 wt.% metal on carbon and were submitted to a thermal treatment conducted in a tubular oven (MAITEC) under an argon atmosphere at 100 °C for the complete elimination of water, followed by treatment in a H_2 atmosphere at 500 °C for 1 h to reduce the metallic ions. Similar procedures for the preparation of the catalysts were published elsewhere [14,15].

The deposition of the Pt monolayer on the Ru/C and Rh/C nanoparticles was performed by the galvanic displacement by Pt of an underpotentially deposited (UPD) Cu monolayer, according to Adzic's work [16]. First, Cu was deposited from 50 mmol L^{-1} $CuSO_4$ and 0.10 mol L^{-1} H_2SO_4 solutions. The electrodes were then rinsed to remove Cu^{2+} from the solution film, and immersed in a 1.0 mmol L^{-1} K_2PtCl_4 in 50 mmol L^{-1} H_2SO_4 solution under a N_2 atmosphere. Allowing 2 min for Pt to completely replace Cu, the electrodes were then removed from the solution and rinsed again. All these operations were carried out in a multi-compartment cell in a N_2 atmosphere to prevent the oxidation of Cu ad-atoms by contact with atmospheric oxygen. The deposition of a Pt monolayer on the surfaces of different substrates was verified by cyclic voltammetry. The Pt monolayer electrocatalysts are represented by Pt/Ru/C or Pt/Rh/C. The results obtained for the Pt monolayer materials were compared to those obtained for the corresponding Pt alloys, represented by Pt–Ru/C or Pt–Rh/C.

The working electrodes for the preparation of the Pt monolayer and for the electrochemical experiments were composed of the metal/C nanoparticles deposited as an ultra-thin layer on a glassy carbon disk, 5 mm diameter (0.196 cm^2), of a rotating disk electrode. The ultra-thin layers were prepared starting from an aqueous suspension of 1.0 mg mL^{-1} of the metal/C produced by ultrasonically dispersing the powder in pure water [17]. A 13 μL aliquot of the dispersed suspension was pipetted on top of the glassy carbon substrate surface. After the evaporation of water, and the Cu UPD procedure, 10 μL of a diluted Nafion solution (prepared from Aldrich 5% solution) were pipetted on the electrode surface in order to attach the catalytic particles on the disk electrode substrate and, after that, dried under vacuum. All the electrochemical experiments were carried out in 0.1 mol L^{-1} $HClO_4$ or 0.1 mol L^{-1} $HClO_4$/0.5 mol L^{-1} CH_3CH_2OH solutions, prepared from high purity reagents (Merck) and water purified in a Milli-Q (Millipore) system. A large area platinum screen served as counter electrode and a reversible hydrogen electrode (RHE) in 0.5 mol L^{-1} $HClO_4$ was used as reference. Cyclic voltammetry and cronoamperometric measurements were recorded in the potentiostatic mode using a 1287A Solartron potentiostat, under controlled temperatures of 25 and 60 ± 0.1 °C by using a Hakee-K20 thermostat.

In situ XANES (X-ray absorption near-edge structure) measurements were performed in the Pt L_3 absorption edge using a home-built spectroelectrochemical cell [18]. The working electrodes consisted of pellets formed with the dispersed catalysts agglutinated with Nafion (ca. 5 wt.%) and containing 6 mg cm^{-2} (Pt loading). The counter electrode was a Pt screen cut in the center in order to allow the free passage of the X-ray beam. The electrolyte was 0.50 mol L^{-1} H_2SO_4 confined in a chamber using an o-ring, and a reversible hydrogen electrode in the same electrolyte was used as reference. The experiments were carried out at 400 and 900 mV vs. RHE, after cycling the electrodes in the range 50–900 mV. Results presented here correspond to the average of at least two independent measurements. All experiments were conducted at the XAFS1 beam line in the Brazilian Synchrotron Light Laboratory (LNLS), Brazil. The data analysis was done according to procedures described in detail in literature [19,20]. Briefly, the XANES (X-ray absorption near-edge structure) spectra were first corrected for the background absorption by fitting the pre-edge data (from −60 to −20 eV below the edge) to a linear formula, followed by extrapolation and subtraction from the data over the energy range of interest. Next, the spectra were calibrated for the edge position using the second derivative of the inflection points at the edge jump of the data from the reference channel. Finally, the spectra were normalized, taking as reference the inflection points of one of the extended X-ray absorption fine structure (EXAFS) oscillations.

In order to compare the intrinsic activities of different catalysts, the currents obtained from the electrochemical half-cell experiments were normalized per total surface active area obtained by stripping of a monolayer of CO and considering a charge of 420 μC cm^{-2} [21]. For this purpose, the CO saturation coverage on the catalysts was achieved by bubbling CO for 10 min at 50 mV followed by bubbling N_2 for 20 min in order to eliminate dissolved CO.

3. Results and discussion

Fig. 1 presents the cyclic voltammograms at a scan rate of 10 mV s^{-1} in 0.1 mol L^{-1} $HClO_4$ for the Pt/Ru/C and Pt/Rh/C materials, obtained after the Pt deposition. The currents are normalized by the geometric surface area. Results show the typical behavior regarding the hydrogen and the oxide regions of Pt in the materials in acid solutions [22]. In the case of Pt/Ru/C, a large value of the double-layer charging current is

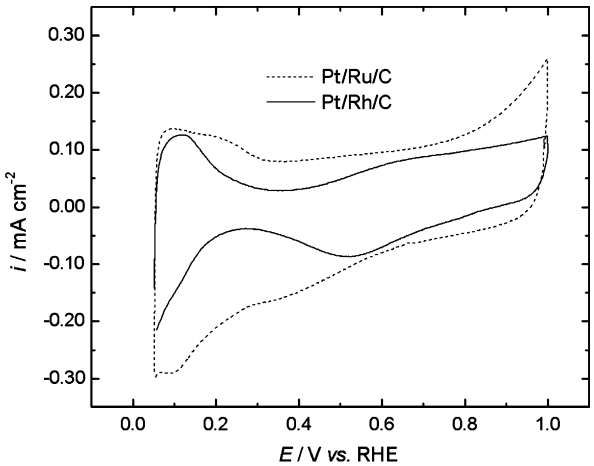

Fig. 1. Cyclic voltammograms obtained for the Pt/Ru/C and Pt/Rh/C electrocatalysts in 0.1 mol L^{-1} $HClO_4$ at 10 mV s^{-1} and 25 °C.

observed, and this is attributed to the presence of Ru-oxides, increasing the electrode capacitance. The hydrogen region in the Pt–Ru/C material is also modified in comparison to that region for pure Pt, and this is due to the formation of oxygenated species on the Ru atoms, in this potential range [23]. In the case of the Pt/Rh/C, the hydrogen adsorption/desorption profile is characterized by large single peaks [24]. So, in both cases, the cyclic voltammogram results evidence some exposition of the Ru and/or Rh substrates to the electrolyte, which evidences the formation of a non-compact full Pt monolayer on Ru/C and Rh/C.

The electronic characterization of platinum of the electrocatalysts was investigated by *in situ* XANES at different electrode potentials. The spectra at the Pt L_3 edge for the Pt/Ru/C and Pt/Rh/C materials are shown in Fig. 2a and b, respectively. Results for Pt/C E-TEK are included for comparison. The absorption at the Pt L_3 edge (11.564 eV) corresponds to $2p_{3/2}$–5d electronic transitions and the magnitude of the absorption hump, or white line, located a few eV past the edge is directly related to the occupancy of the 5d electronic states. The higher the hump the lower is the occupancy and vice versa. For pure Pt/C it is observed that the Pt 5d band vacancy increases considerably by increasing the potential. This phenomenon is attributed to the emptying of the Pt 5d band, in agreement with the presence of an electron withdrawing effect of the oxygen present in a well-known surface oxide layer formed above 800 mV on the catalyst particle surface, due to the water activation [25]. On the other hand, the Pt occupancy on the Pt/Ru/C and Pt/Rh/C materials does not change appreciably by increasing the electrode potential. This may be ascribed to some electronic interaction and the Pt lattice contraction induced by Ru or Rh atoms (smaller atomic radii) leading to a broader Pt band. This phenomenon may reduce the Pt density of states close to the Fermi level, leading to a

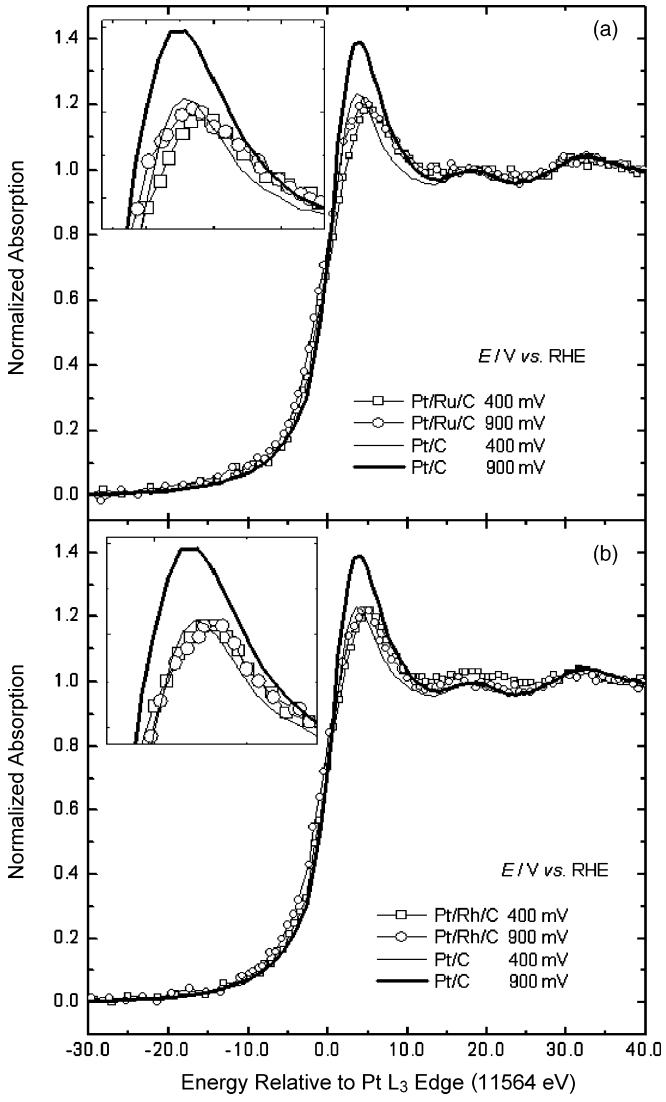

Fig. 2. *In situ* XANES spectra at the Pt L_3 edge for (a) Pt/Ru/C and (b) Pt/Rh/C electrocatalysts in 0.5 mol L^{-1} H_2SO_4 at 0.40 and 0.90 V vs. RHE and at 25 °C. Results for Pt/C E-TEK are included for comparison.

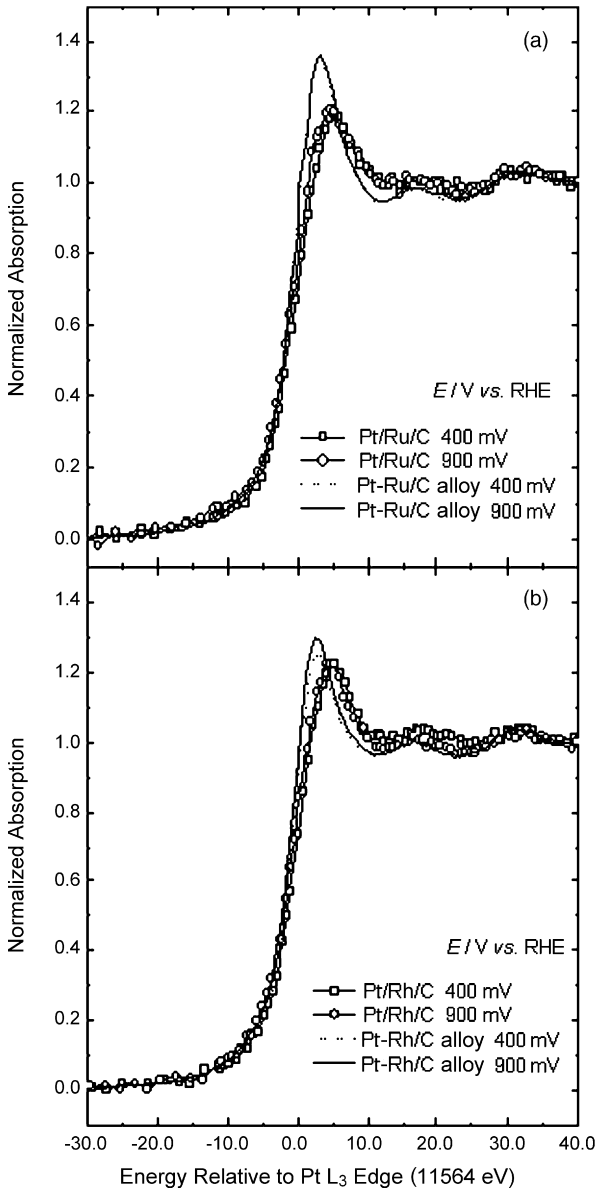

Fig. 3. *In situ* XANES spectra at the Pt L_3 edge for (a) Pt/Ru/C and (b) Pt/Rh/C electrocatalysts in 0.5 mol L^{-1} H_2SO_4 at 0.40 and 0.90 V vs. RHE and at 25 °C, compared to those for Pt–Ru/C (dashed line) and Pt–Rh/C (dotted line) alloys.

lowering of the Pt d-band center, which reduces the adsorption strength of adsorbates on the Pt surface [11].

Fig. 3a and b presents a comparison of the *in situ* XANES spectra for the Pt monolayer materials with those obtained for Pt–Ru/C and Pt–Rh/C alloy catalysts, respectively. The results show a significant difference in the absorption hump, where it can be observed that the vacancy of the Pt 5d level is larger in the case of the alloys. This may arises from the electron withdrawing effect from Pt due to a higher Pt–Ru and/or Pt–Rh electronic interaction due to the preparation method, which involves a thermal treatment at high temperature to reduce the metal ions. Also, there is no significant change in the white line for the alloys by increasing the electrode potential, indicating a lower Pt reactivity, as in the case of the Pt monolayer materials. Thus, based on these results, and although the Ru/C and/or Rh/C substrates do not promote a larger Pt 5d vacancy on the Pt of the Pt monolayer, their geometric effect and electronic interactions are sufficient for lowering the Pt d-band center and, consequently, decrease the Pt reactivity for adsorbates.

Fig. 4a and b compares the CO stripping at 10 mV s^{-1} for the different electrocatalysts at 25 and 60 °C, respectively. Results for the Pt–Ru/C and Pt–Rh/C alloys are included for comparison. Lower overpotentials are observed for the materials with Ru, which is an evidence of a facilitated CO oxidation on Ru-containing materials [9]. This is ascribed to the lower Pt–CO adsorption strength on these catalysts, as evidenced by theoretical calculations [26], and by the reduced reactivity of the Pt atoms, demonstrated by the XANES results.

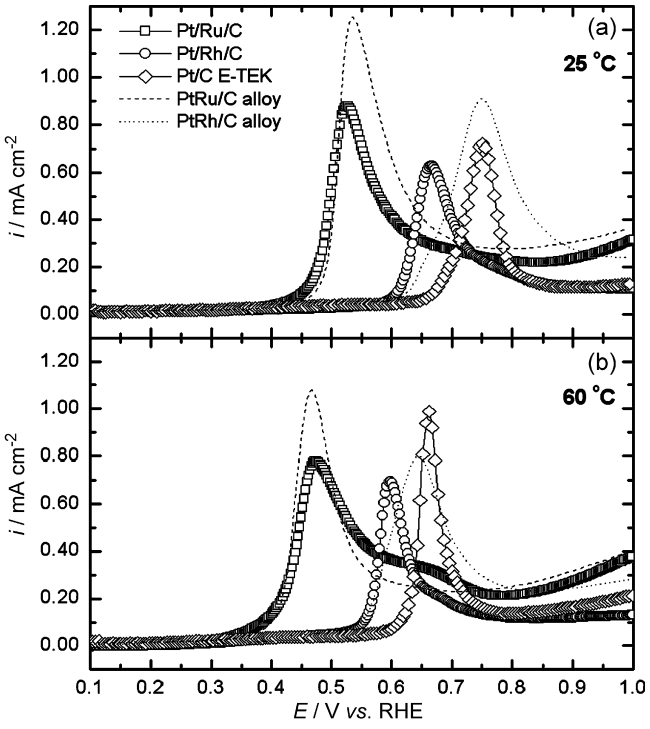

Fig. 4. Linear sweep voltammetry of the adsorbed CO stripping on the Pt/Ru/C and Pt/Rh/C monolayer materials at (a) 25 and (b) 60 °C in 0.10 mol L^{-1} $HClO_4$. Scan rate of 10 mV s^{-1} and adsorption potential of 0.05 V vs. RHE. Results for Pt–Ru/C (dashed line) and Pt–Rh/C (dotted line) are included for comparison.

Also, the faster CO oxidation may be due to a favored bi-functional mechanism, as proposed before [27]. In this mechanism, the role of Ru atoms is to provide OH groups, or oxygenated species, for the coupling with the CO adsorbed species on Pt, which leads to the formation of CO_2. In the case of the Pt/Rh/C material, it is also seen a shift of the onset potentials for CO oxidation to lower potential values. However, the shift to lower onset potentials is not as pronounced as that observed for Pt/Ru/C. As discussed before [4], the enhanced CO oxidation on Pt/Rh/C seems to be related to more intrinsic electrocatalytic properties, produced by electronic effects on the Pt atoms, and so, the mechanism where Rh promotes the availability of oxygen necessary for the oxidation of CO takes place at a lower extent. Comparing the CO stripping results on Pt/Ru/C and Pt/Rh/C with those on the Pt–Ru/C and Pt–Rh/C alloys, lower onset potentials are observed for the Pt-monolayer materials. This may be attributed to improved geometric and electronic properties induced by the interaction of the Pt monolayer with the Ru/C and Rh/C substrates, conducting to a lower Pt–CO adsorption strength. Also, it may be ascribed to a larger number of active Pt sites at the particle surface for the water activation (due to larger number of surface defects), which promotes a faster CO–O coupling.

The electrocatalytic activities for the electro-oxidation of ethanol on the Pt-monolayer materials were compared by cyclic voltammetry and cronoamperometric measurements. Fig. 5a

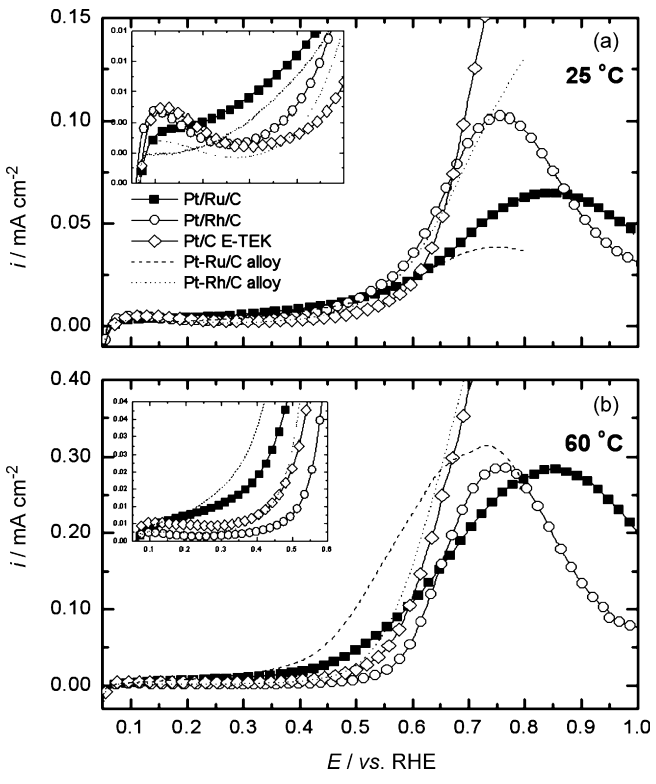

Fig. 5. Anodic sweep of the cyclic voltammetry for the ethanol oxidation on the Pt/Ru/C and Pt/Rh/C monolayer materials at (a) 25 and (b) 60 °C in 0.50 mol L^{-1} C_2H_5OH/0.10 mol L^{-1} $HClO_4$ solution. Scan rate of 10 mV s^{-1} 1 and adsorption potential of 0.05 V vs. RHE. Inset: Detail of the lower potential regions. Results for Pt–Ru/C (dashed line) and Pt–Rh/C (dotted line) are included for comparison.

and b presents the anodic scan of the cyclic voltammetries at 25 and 60 °C, respectively, for the Pt-monolayer catalysts, with the currents normalized by the active surface area obtained from the charge of CO stripping. Results for Pt–Ru/C, Pt–Rh/C alloys and for Pt/C E-TEK are included for comparison. The insets in the figures show details of the region of low overpotentials. The curves at 25 °C show slightly increased activities for the Pt-monolayer materials, in relation to those for the alloys and also a higher catalytic activity for the bimetallic materials, when compared to that for Pt/C. But at high overpotentials, Pt/C shows higher currents. The anodic curves at 60 °C indicate higher activity for the Pt alloys, mainly for Pt–Ru/C. The activity trends at 500 mV are better compared by quasi-steady state techniques and were monitored by cronoamperometric measurements. Fig. 6a and b shows the curves for electro-oxidation of ethanol at 25 and 60 °C, respectively. Cronoamperometric curves indicate much higher activity for the materials containing Ru. Pt/Rh/C and Pt–Rh/C alloys showed a similar activity, and higher than that for Pt/C at 25 °C. Also, it is observed an increased activity at 60 °C for the Pt–Rh/C alloy.

The lower onset potentials for CO and ethanol electro-oxidation on the Ru-containing materials are in favor of the proposal that the Ru atoms act by facilitating the stripping of CO through a favorable electronic effect on Pt, and by providing oxygenated species for the CO–O coupling. This leads to the formation of CO_2 and some oxygenated intermediates at low overpotentials [2]. On the other hand, it can be noted that the shift to lower onset potentials for CO oxidation on the Rh-containing catalysts is not as pronounced as that observed for Ru-containing

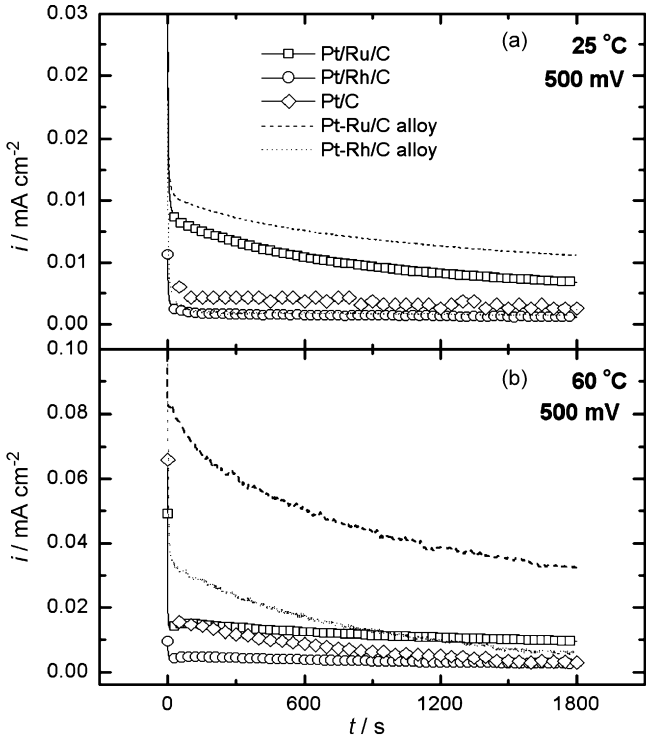

Fig. 6. Cronoamperommetric curves for the ethanol oxidation on the Pt/Ru/C and Pt/Rh/C monolayer materials at (a) 25 and (b) 60 °C in 0.50 mol L^{-1} C_2H_5OH/0.10 mol L^{-1} $HClO_4$ solution at 500 mV. Results for Pt–Ru/C (dashed line) and Pt–Rh/C (dotted line) are included for comparison.

materials. It was previously proposed [4] that the role of Rh atoms is more correlated to intrinsic electrocatalytic property (changes in the Pt 5d band). However, in the case of the ethanol electrocatalysis, Rh atoms clearly increase the C–C bond dissociation, as it was indicated by the higher CO_2/acetic acid ratio. In addition, as the present electrocatalysts are formed by clusters of Pt on the Ru and/or Rh nanoparticles, it may contain large amount of defect and steps at the surface, which would enhance the C–C bond breaking.

It must be stressed here that although the Pt/Ru/C and Pt/Rh/C materials contain very low amounts of Pt, they show very good activities, which can even exceed the activity of Pt alloys at 25 °C at low overpotentials. The charges associated with the Cu UPD on the Ru/C and Rh/C substrates were 3.0 and 2.34 mC cm^{-2}, respectively. This results in a Pt loading of 1.5 and 1.2 μg cm^{-2}, which is very lower than that of Pt/C nanoparticles (13.0 μg cm^{-2}). Therefore, the enhanced activity of the Pt monolayers on Ru/C and Rh/C may be the result of a better tuning of its geometric and electronic properties induced by the interaction with the substrates. The enhanced kinetics at lower overpotentials may be associated with the lower Pt–CO adsorption strength, leading to a faster CO oxidation from the Pt surface. Also, it may result from the geometric configuration of the Pt at the surface, which may present higher number of defects, which promotes faster water activation. On the other hand, experiments at 60 °C point out to higher electrochemical currents for the alloys in relation to the monolayer materials. This would be ascribed to the presence of a larger number of Ru and Rh atoms at the particle surface in the case of the alloys, which may enhances the bi-functional effect. Also, it may be mentioned that higher temperatures may favor the adsorption of ethanol on Ru, and maybe also on Rh [28], which would conduct to a faster electro-oxidation of ethanol. Another hypothesis for the lower activity of the Pt-monolayer materials, in comparison to the alloys, is that the positive effect of the core–shell structures at 25 °C is somewhat cancelled at 60 °C due to the partial destruction of the Pt monolayer or some formation of very large Pt clusters at the nanoparticle surface. These phenomena and the products of the ethanol electro-oxidation on the Pt-monolayer materials are under investigation in our laboratory.

4. Conclusions

XANES measurements show a reduced 5d band vacancy at higher potentials of Pt atoms at the surface of Ru/C and Rh/C substrates, which indicates lower formation of Pt-oxides. This implicates in a decreased adsorption strength of adsorbates, as CO, on the Pt atoms, increasing the CO oxidation rate. Pt/Ru/C and Pt/Rh/C electrocatalysts produced a decrease in the onset potential for the CO and ethanol electro-oxidation. At 25 °C, the onset potentials for ethanol electro-oxidation were even lower than those for the Pt–Ru/C and Pt–Rh/C alloys. This was ascribed to a better tuning of the Pt monolayer geometric and electronic features to the requirements of the reaction. On the other hand, the alloys were more active at 60 °C, and this was attributed to the presence of higher number of Ru and/or Rh

atoms at the surface of the alloys, leading to an enhanced bifunctional mechanism and C–H bond activation, and/or stronger alcohol adsorption. Also, it was considered a partial destruction of the Pt monolayer, as the cause of their lower activity at 60 °C, when compared to that of the alloys.

Therefore, it was shown an enhanced catalysis for ethanol oxidation on materials consisting of a Pt monolayer deposited on non-noble metal substrates (core–shell nanoparticles). So, it is possible to develop electrocatalysts, with the Cu UPD method, containing only a fractional amount of Pt and with larger activity than those of the largely used carbon-supported Pt and Pt alloy electrocatalysts. Further work is in progress in our laboratory to investigate the products of the ethanol electrooxidation on the Pt-monolayer materials.

Acknowledgments

The authors thank the Fundação de Amparo à Pesquisa do Estado de São Paulo (FAPESP), the Conselho Nacional de Desenvolvimento Científico e Tecnológico (CNPq), the Coordenação de Aperfeiçoamento de Pessoal de Nível Superior (CAPES) for financial support, and the Brazilian Synchrotron Light Laboratory (LNLS) for the XAS experiments.

References

[1] W. Vielstich, H.A. Gasteiger, A. Lamm, Handbook of Fuel Cells—Fundamentals, Technology and Applications, Wiley, Chichester, 2003.
[2] G.A. Câmara, R.B. de Lima, T. Iwasita, J. Electroanal. Chem. 585 (2005) 128.
[3] G.A. Camara, T. Iwasita, J. Electroanal. Chem. 578 (2005) 315.
[4] J.P.I. de Souza, S.L. Queiroz, K. Bergamaski, E.R. Gonzalez, F.C. Nart, J. Phys. Chem. B 106 (2002) 9825.
[5] C. Lamy, S. Rousseau, E.M. Belgsir, C. Coutanceau, J.-M. Leger, Electrochim. Acta 49 (2004) 3901.
[6] J.-M. Leger, S. Rousseau, C. Coutanceau, F. Hahn, C. Lamy, Electrochim. Acta 50 (2005) 5118.
[7] M.H. Shao, R.R. Adzic, Electrochim. Acta 50 (2005) 2415.
[8] J.X. Wang, N.S. Marinkovic, H. Zajonz, B.M. Ocko, R.R. Adzic, J. Phys. Chem. 105 (2001) 2809.
[9] K. Sasaki, J.X. Wang, M. Balasubramanian, J. McBreen, F. Uribe, R.R. Adzic, Electrochim. Acta 49 (2004) 3873.
[10] B. Hammer, J.K. Nørskov, Surf. Sci. 343 (1995) 211.
[11] J.R. Kitchin, J.K. Nørskov, M.A. Barteau, G. Chen, J. Chem. Phys. 120 (2004) 10240.
[12] B. Hammer, J.K. Nørskov, Adv. Catal. 45 (2000) 71.
[13] J. Greeley, J.K. Nørskov, M. Mavrikakis, Annu. Rev. Phys. Chem. 53 (2002) 319.
[14] G. Camara, M.J. Giz, V.A. Paganin, E.A. Ticianelli, J. Electroanal. Chem. 537 (2002) 21.
[15] J. Zhang, F.H.B. Lima, M.H. Shao, K. Sasaki, J.X. Wang, J. Hanson, R.R. Adzic, J. Phys. Chem. B 109 (2005) 22701.
[16] J. Zhang, Y. Mo, M.B. Vukmirovic, R. Klie, K. Sasaki, R.R. Adzic, J. Phys. Chem. B 108 (2004) 10955.
[17] T.J. Schmidt, H.A. Gasteiger, G.D. Stäb, P.M. Urban, D.M. Kolb, R.J. Behm, J. Electrochem. Soc. 145 (1998) 2354.
[18] J. McBreen, W.E. O'Grady, K.I. Pandya, R.W. Roffman, D.E. Sayers, Langmuir 3 (1987) 428.
[19] K.I. Pandya, R.W. Roffman, J. McBreen, W.E. O'Grady, J. Electrochem. Soc. 137 (1990) 383.
[20] J.B.A.C. van Zon, D.C. Konigsberger, H.F.J. Van't Blik, D.E. Sayers, J. Chem. Phys. 82 (1985) 5742.
[21] J.P.I. Souza, T. Iwasita, F.C. Nart, W. Vielstich, J. Appl. Electrochem. 30 (1999) 43.
[22] U.A. Paulus, A. Wokaum, G.G. Sherer, T.J. Schmidt, V. Stamenkovic, N.M. Markovic, P.N. Ross, Electrochim. Acta 47 (2002) 3787.
[23] H.A. Gasteiger, N. Markovic, P.N. Ross Jr., E.J. Cairns, J. Phys. Chem. 98 (1994) 617.
[24] S.S. Gupta, J. Datta, J. Electroanal. Chem. 594 (2006) 65.
[25] S. Mukerjee, S. Srinivasan, M.P. Soriaga, J. McBreen, J. Electrochem. Soc. 142 (1995) 1409.
[26] B. Hammer, Y. Morikawa, J.K. Nørskov, Phys. Rev. Lett. 76 (1996) 2141.
[27] F. Maillard, G.-Q. Lu, A. Wiechowiski, U. Stimming, J. Phys. Chem. B 109 (2005) 16230.
[28] H.A. Gasteiger, N. Markovic, P.N. Ross, E.J. Cairns, J. Electrochem. Soc. 141 (1994) 1795.